Pergamon

Int. J. Heat Mass Transfer. Vol. 37, No. 4, pp. 699–704, 1994

0017-9310/94 $6.00+0.00

TECHNICAL NOTES

Laminar mixed convection on horizontal flat plates with variable surface heat flux

W. R. RISBECK, T. S. CHEN and B. F. ARMALY
Department of Mechanical and Aerospace Engineering and Engineering Mechanics,
University of Missouri-Rolla, Rolla, MO 65401, U.S.A.

(*Received* 14 *June* 1993 *and in final form* 6 *September* 1993)

INTRODUCTION

PAST STUDIES on mixed convection in external flow have covered different geometries, such as vertical plates [1, 2], inclined plates [3, 4], and horizontal plates [5–10]. Ramachandran *et al.* [6] studied mixed convection over a horizontal plate under uniform wall temperature for the entire mixed convection regime, by analyzing the effect of buoyancy force on forced convection from one end and the effect of forced flow on free convection from the other end. Later, Raju *et al.* [8] employed a single mixed convection parameter, which varies from 0 for pure free convection to 1 for pure forced convection, to analyze the same problem. Very recently, Risbeck *et al.* [10] re-examined the problem for power-law variation in the wall temperature by using a different single mixed convection parameter that also covers the entire mixed convection regime and varies from 0 to 1 (from pure free convection to pure forced convection). The present note is an extension of the latter work [10] to the power-law variation in surface heat flux, again using a single mixed convection parameter that covers the entire regime of mixed convection. Numerical results are presented for a range of Prandtl numbers under different levels of heating. Correlation equations for the local and average Nusselt numbers are also given.

ANALYSIS

Consider laminar mixed convection flow over a semi-infinite horizontal flat plate with surface heat flux that varies as $q_w(x) = bx^m$, where b and m are real constants. The free stream temperature is T_∞ and the free stream velocity parallel to the plate is u_∞. The x coordinate is measured from the leading edge of the plate and the y coordinate is measured normal to the plate. The velocity components in the x and y directions are u and v, respectively. Under the Boussinesq approximation, the governing boundary-layer equations for a constant-property fluid may be written as [5, 10]

$$\frac{\partial u}{\partial x}+\frac{\partial v}{\partial y}=0 \tag{1}$$

$$u\frac{\partial u}{\partial x}+v\frac{\partial u}{\partial y}=\pm g\beta\frac{\partial}{\partial x}\int_y^\infty (T-T_\infty)\,\mathrm{d}y+\nu\frac{\partial^2 u}{\partial y^2} \tag{2}$$

$$u\frac{\partial T}{\partial x}+v\frac{\partial T}{\partial y}=\alpha\frac{\partial^2 T}{\partial y^2}. \tag{3}$$

The corresponding boundary conditions are

$$u=v=0,\quad -k\frac{\partial T}{\partial y}=q_w(x)=bx^m \quad \text{at} \quad y=0$$
$$u\to u_\infty,\quad T\to T_\infty \quad \text{as} \quad y\to\infty. \tag{4}$$

The first term on the right-hand side of equation (2) is the buoyancy-induced streamwise pressure gradient, and the plus and minus signs refer, respectively, to flow above and below the plate.

The system of equations (1)–(4) can be transformed into a dimensionless form by introducing the following non-dimensional quantities

$$\eta=\frac{y}{x}Re_x^{1/2}\chi^{*-1},\quad \chi^*=\frac{Re_x^{1/2}}{Re_x^{1/2}+Gr_x^{*1/6}} \tag{5}$$

$$f(\chi^*,\eta)=\frac{\psi}{\nu Re_x^{1/2}}\chi^*,\quad \theta(\chi^*,\eta)=\frac{(T-T_\infty)Re_x^{1/2}}{\chi^*[q_w(x)x/k]} \tag{6}$$

where χ^* is a nonsimilar mixed convection parameter, with $Re_x = u_\infty x/\nu$ and $Gr_x^* = g\beta q_w(x)x^4/(k\nu^2)$ denoting, respectively, the local Reynolds and modified Grashof numbers, η is a pseudo-similarity variable, $f(\chi^*,\eta)$ is the reduced stream function, and $\theta(\chi^*,\eta)$ is the dimensionless temperature. The stream function $\psi(x,y)$ satisfies the continuity equation with $u=\partial\psi/\partial y$ and $v=-\partial\psi/\partial x$. It is noted here that the mixed convection parameter χ^* varies from 0 for pure free convection to 1 for pure forced convection. This transformation yields

$$f'''+\frac{1}{6}[3+(m+1)(1-\chi^*)]ff''-\frac{(m+1)}{3}(1-\chi^*)f'^2$$
$$\pm\frac{1}{6}(1-\chi^*)^6\Big\{[3-(m+1)(1-\chi^*)]\eta\theta$$
$$+[6(m+1)-2(m+1)(1-\chi^*)]G-(m+1)\chi^*(1-\chi^*)\frac{\partial G}{\partial\chi^*}\Big\}$$
$$=\frac{m+1}{6}\chi^*(1-\chi^*)\left\{f''\frac{\partial f}{\partial\chi^*}-f'\frac{\partial f'}{\partial\chi^*}\right\} \tag{7}$$

$$\frac{\theta''}{Pr}+\frac{1}{6}[3+(m+1)(1-\chi^*)]f\theta'$$
$$-\frac{1}{6}[3(2m+1)-(m+1)(1-\chi^*)]f'\theta$$
$$=\frac{m+1}{6}\chi^*(1-\chi^*)\left\{\theta'\frac{\partial f}{\partial\chi^*}-f'\frac{\partial\theta}{\partial\chi^*}\right\} \tag{8}$$

$$G'+\theta=0 \tag{9}$$

$$f'(\chi^*,0)=0,\quad f'(\chi^*,\infty)=\chi^{*2}$$
$$[3+(m+1)(1-\chi^*)]f(\chi^*,0)$$
$$-(m+1)\chi^*(1-\chi^*)\frac{\partial f}{\partial\chi^*}(\chi^*,0)=0$$
$$\theta'(\chi^*,0)=-1,\quad \theta(\chi^*,\infty)=0,\quad G(\chi^*,\infty)=0. \tag{10}$$

In equations (7)–(10), the primes denote partial differentiation with respect to η, Pr is the Prandtl number, and

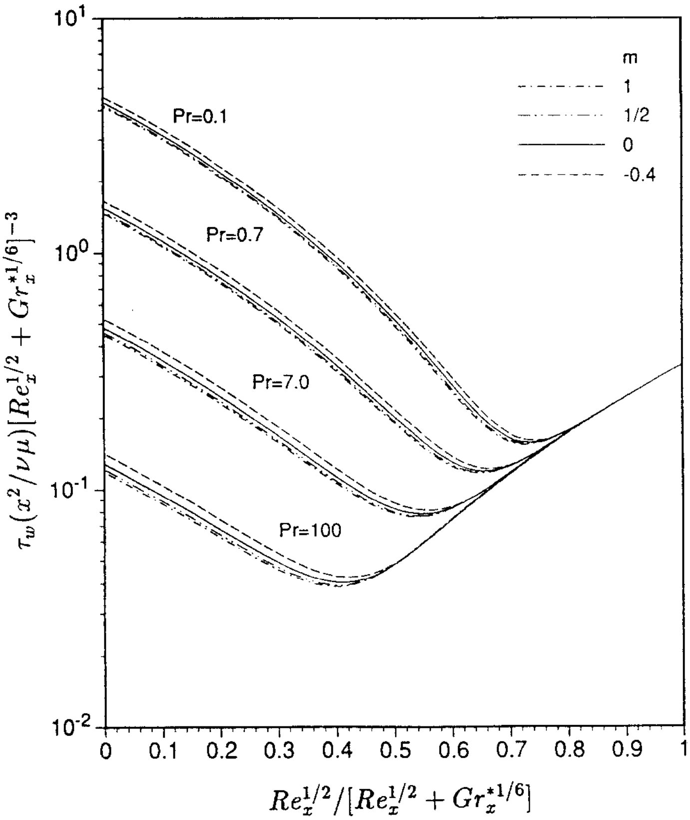

FIG. 1. Results for the local wall shear stress, $\tau_w(x^2/\nu\mu)[Re_x^{1/2}+Gr_x^{*1/6}]^{-3}$.

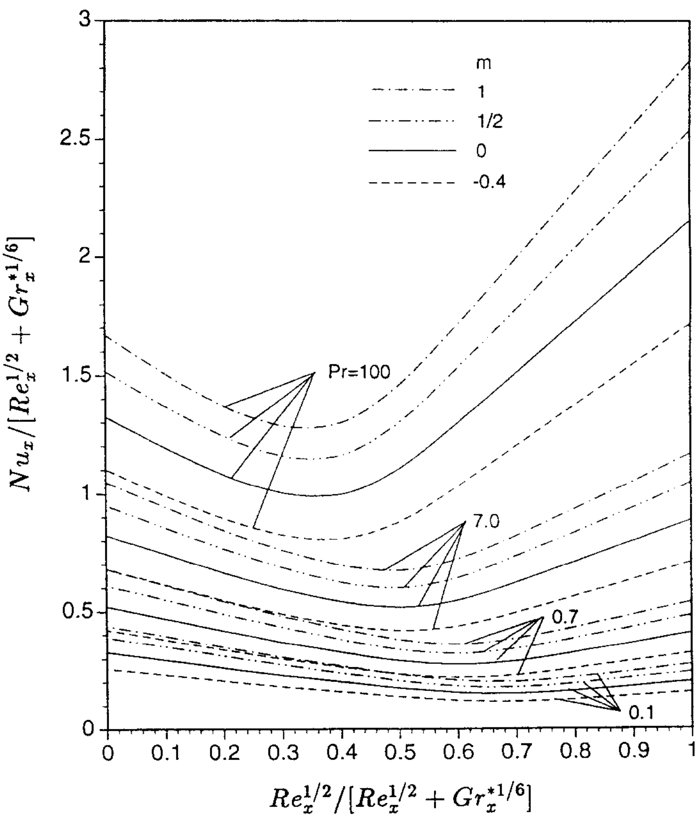

FIG. 2. Results for the local Nusselt number, $Nu_x/(Re_x^{1/2}+Gr_x^{*1/6})$.

$$G = \int_{\eta}^{\infty} \theta \, d\eta. \tag{11}$$

The plus/minus sign in front of the fourth term in equation (7) now stands for buoyancy assisting/opposing flow.

The physical quantities of interest include the axial velocity distribution, the temperature profile $\theta(\chi^*, \eta)/\theta(\chi^*, 0) = (T - T_\infty)/(T_w - T_\infty)$, the local Nusselt number $Nu_x = hx/k$ (where $h = q_w/(T_w - T_\infty)$ is the local heat transfer coefficient, with $q_w = -k(\partial T/\partial y)_{y=0}$), and the local wall shear stress $\tau_w = \mu(\partial u/\partial y)_{y=0}$. In terms of the transformation variables, the expressions for u/u_∞, Nu_x, and τ_w can be written as

$$u/u_\infty = f'(\chi^*, \eta)/\chi^{*2} \tag{12}$$

$$\frac{Nu_x}{Re_x^{1/2} + Gr_x^{*1/6}} = \frac{1}{\theta(\chi^*, 0)} \tag{13}$$

and

$$\frac{\tau_w(x^2/\mu\nu)}{(Re_x^{1/2} + Gr_x^{*1/6})^3} = f''(\chi^*, 0). \tag{14}$$

Also of interest is the average Nusselt number $\overline{Nu}_L = \bar{h}L/k$, where $\bar{h}$ is the average heat transfer coefficient over the plate length L. It has the expression

$$\frac{\overline{Nu}_L}{Re_L^{1/2} + Gr_L^{*1/6}} = \frac{6}{m+1} \chi_L^* \left\{ \frac{\chi_L^*}{1 - \chi_L^*} \right\}^{3/(m+1)} \times \int_{\chi_L^*}^{1} \frac{[1/\theta(\chi^*, 0)]}{\chi^{*3}} \left\{ \frac{1 - \chi^*}{\chi^*} \right\}^{(2-m)/(m+1)} d\chi^* \tag{15}$$

where Re_L, Gr_L^*, and χ_L^* are Re_x, Gr_x^*, and χ^* at $x = L$. The corresponding $\overline{Nu}_L$ expression for $\chi_L^* = 0$ (pure free convection with $Re_L = 0$) can be found as

$$\left(\frac{\overline{Nu}_L}{Re_L^{1/2} + Gr_L^{*1/6}} \right)_{\chi_L^* \to 0} = \overline{Nu} Gr_L^{*-1/6} = \frac{6}{m+4} \left(\frac{1}{\theta(0, 0)} \right) \tag{16}$$

and that for $\chi_L^* = 1$ (pure forced convection with $Gr_L^* = 0$) has the form

$$\left(\frac{\overline{Nu}_L}{Re_L^{1/2} + Gr_L^{*1/6}} \right)_{\chi_L^* \to 1} = \overline{Nu} Re_L^{-1/2} = 2 \left(\frac{1}{\theta(1, 0)} \right). \tag{17}$$

RESULTS AND DISCUSSION

Equations (7)–(10) were solved by a weighted finite-difference method as described in ref. [10]. Numerical results were obtained for buoyancy assisting flow covering $0.1 \leqslant Pr \leqslant 100$ and $-0.4 \leqslant m \leqslant 1.0$. This range of m values lies within the physical limits $-1 \leqslant m \leqslant 1$ (see Gebhart [11]). It is noted here that a step size of $\Delta\eta = 0.02$ gave accurate results for $0.1 \leqslant Pr \leqslant 7$. However, a step size of $\Delta\eta = 0.01$ was required for $Pr = 100$. The value of η_∞ ranged from 10 to 20. The choice of a step size of $\Delta\chi^* = 0.05$ was sufficient for all the cases considered. Results are presented for buoyancy assisting flows.

The effects of Prandtl number Pr and the exponent value m on the velocity and temperature profiles are similar to those for the case of power-law wall temperature variation [10] and, to conserve space, they are not illustrated. The local wall shear stress parameter $\tau_w(x^2/\nu\mu)[Re_x^{1/2} + Gr_x^{*1/6}]^{-3}$ and the local Nusselt number parameter $Nu_x/[Re_x^{1/2} + Gr_x^{*1/6}]$ as a function of $\chi^* = Re_x^{1/2}/[Re_x^{1/2} + Gr_x^{*1/6}]$ are shown, respectively, in Figs. 1 and 2 for values of the exponent $m = -0.4$, 0, 1/2, and 1, and Prandtl numbers of $Pr = 0.1$, 0.7, 7.0, and 100. Their numerical values are listed, respectively, in Tables 1 and 2. As can be seen from the figures, for a given m, values for both the wall shear stress parameter and the Nusselt

Table 1. Results for the local wall shear stress $\tau_w(x^2/\mu\nu)(Re_x^{1/2} + Gr_x^{*1/6})^{-3} = f''(\chi^*, 0)$

	$Pr = 0.1$				$Pr = 0.7$			
	m				m			
χ^*	−0.4	0	1/2	1	−0.4	0	1/2	1
0	4.5812	4.3317	4.2109	4.1518	1.6605	1.5493	1.4961	1.4711
0.1	3.3358	3.1537	3.0658	3.0228	1.2100	1.1285	1.0895	1.0712
0.2	2.3372	2.2085	2.1460	2.1150	0.8495	0.7917	0.7638	0.7504
0.3	1.5595	1.4719	1.4284	1.4061	0.5698	0.5304	0.5108	0.5012
0.4	0.9766	0.9196	0.8897	0.8735	0.3621	0.3364	0.3232	0.3164
0.5	0.5631	0.5276	0.5075	0.4959	0.2188	0.2034	0.1952	0.1909
0.6	0.2972	0.2773	0.2654	0.2584	0.1379	0.1307	0.1269	0.1250
0.7	0.1710	0.1641	0.1602	0.1581	0.1266	0.1254	0.1250	0.1249
0.8	0.1756	0.1755	0.1756	0.1757	0.1718	0.1722	0.1726	0.1730
0.9	0.2429	0.2433	0.2436	0.2438	0.2428	0.2431	0.2434	0.2436
1.0	0.3321	0.3321	0.3321	0.3321	0.3321	0.3321	0.3321	0.3321
	$Pr = 7.0$				$Pr = 100$			
	m				m			
χ^*	−0.4	0	1/2	1	−0.4	0	1/2	1
0	0.5253	0.4815	0.4597	0.4493	0.1423	0.1289	0.1221	0.1187
0.1	0.3835	0.3514	0.3355	0.3278	0.1041	0.0943	0.0894	0.0869
0.2	0.2709	0.2483	0.2370	0.2316	0.0745	0.0677	0.0642	0.0625
0.3	0.1849	0.1697	0.1620	0.1583	0.0535	0.0491	0.0468	0.0457
0.4	0.1235	0.1140	0.1091	0.1067	0.0429	0.0404	0.0393	0.0387
0.5	0.0877	0.0827	0.0802	0.0789	0.0484	0.0478	0.0477	0.0479
0.6	0.0845	0.0832	0.0828	0.0827	0.0738	0.0742	0.0746	0.0750
0.7	0.1165	0.1169	0.1173	0.1177	0.1152	0.1157	0.1163	0.1167
0.8	0.1712	0.1717	0.1721	0.1725	0.1711	0.1716	0.1721	0.1724
0.9	0.2427	0.2431	0.2434	0.2436	0.2428	0.2431	0.2434	0.2436
1.0	0.3321	0.3321	0.3321	0.3321	0.3321	0.3321	0.3321	0.3321

Table 2. Results for the local Nusselt number $Nu_x/(Re_x^{1/2}+Gr_x^{*1/6}) = 1/\theta(\chi^*, 0)$

	$Pr = 0.1$				$Pr = 0.7$			
	m				m			
χ^*	−0.4	0	1/2	1	−0.4	0	1/2	1
0	0.2577	0.3276	0.3898	0.4380	0.4216	0.5216	0.6099	0.6785
0.1	0.2316	0.2944	0.3508	0.3936	0.3790	0.4670	0.5491	0.6100
0.2	0.2059	0.2617	0.3120	0.3497	0.3377	0.4178	0.4894	0.5432
0.3	0.1811	0.2300	0.2741	0.3071	0.2985	0.3693	0.4321	0.4799
0.4	0.1577	0.2003	0.2381	0.2671	0.2629	0.3256	0.3799	0.4231
0.5	0.1370	0.1741	0.2060	0.2322	0.2343	0.2910	0.3384	0.3791
0.6	0.1213	0.1547	0.1824	0.2070	0.2192	0.2744	0.3204	0.3605
0.7	0.1156	0.1487	0.1768	0.2008	0.2281	0.2884	0.3406	0.3824
0.8	0.1243	0.1611	0.1933	0.2187	0.2564	0.3248	0.3846	0.4310
0.9	0.1394	0.1806	0.2169	0.2451	0.2885	0.3652	0.4323	0.4842
1.0	0.1550	0.2007	0.2410	0.2720	0.3209	0.4059	0.4803	0.5376

	$Pr = 7.0$				$Pr = 100$			
	m				m			
χ^*	−0.4	0	1/2	1	−0.4	0	1/2	1
0	0.6807	0.8244	0.9506	1.0488	1.1022	1.3245	1.5178	1.6704
0.1	0.6124	0.7418	0.8565	0.9442	0.9933	1.1946	1.3709	1.5085
0.2	0.5473	0.6638	0.7666	0.8460	0.8965	1.0817	1.2442	1.3724
0.3	0.4885	0.5940	0.6856	0.7597	0.8256	1.0043	1.1586	1.2870
0.4	0.4416	0.5402	0.6232	0.6950	0.8069	0.9963	1.1588	1.2972
0.5	0.4179	0.5167	0.5996	0.6723	0.8776	1.1007	1.2948	1.4529
0.6	0.4355	0.5457	0.6411	0.7188	1.0261	1.2918	1.5238	1.7082
0.7	0.4933	0.6207	0.7321	0.8196	1.1966	1.5050	1.7745	1.9865
0.8	0.5633	0.7082	0.8351	0.9340	1.3698	1.7206	2.0277	2.2674
0.9	0.6344	0.7969	0.9393	1.0496	1.5432	1.9363	2.2811	2.5485
1.0	0.7057	0.8856	1.0436	1.1653	1.7164	2.1519	2.5344	2.8294

number parameter initially decrease as χ^* increases from 0 until they reach a minimum value and thereafter increase as χ^* increases further to 1.0. The value of the local Nusselt number parameter, Fig. 2, is seen to increase with increasing m for a given value of χ^*, with higher parameter values for larger Prandtl numbers, whereas the value of the local wall shear stress parameter, Fig. 1, decreases with increasing m for a given χ^*, with a lower parameter value for a larger Prandtl number.

The behavior of the curves for the local wall shear stress parameter and the local Nusselt number parameter, as shown in Figs. 1 and 2, does not imply that the wall shear stress and the Nusselt number for mixed convection are lower than those predicted for pure forced convection or pure free convection. For example, consider the case of $Pr = 0.7$, $m = 0$, and $\chi^* = 0.5$. If the Reynolds number is taken as $Re_x = 10^3$ the corresponding modified Grashof number is $Gr_x^* = 10^9$. From Tables 1 and 2 the local wall shear stress $\tau_w(x^2/\nu\mu)$ and the local Nusselt number Nu_x for the case of pure forced convection ($\chi^* = 1$, $Re_x = 10^3$, $Gr_x^* = 0$) are found to be 10 502 and 12.836, respectively. For the case of pure free convection ($\chi^* = 0$, $Gr_x^* = 10^9$, $Re_x = 0$) they are, respectively, 48 993 and 16.494. For mixed convection with $\chi^* = 0.5$ ($Re_x = 10^3$ and $Gr_x^* = 10^9$) their respective values are 51 457 and 18.404. Thus, the predicted values of local wall shear stress and local Nusselt number for mixed convection are actually higher than the respective values predicted for pure forced convection or pure free convection.

The local Nusselt number Nu_x can also be expressed in terms of $Nu_x Re_x^{-1/2}$ vs $Gr_x^* Re_x^{-3}$ in a log–log scale. As shown in Fig. 3, the resulting curves asymptotically approach the straight line limits for pure forced convection ($Gr_x^*/Re_x^3 = 0$) and pure free convection ($Gr_x^*/Re_x^3 \to \infty$).

Correlation equations for the local and average Nusselt numbers in forced convection over a flat plate for $0.1 \leqslant Pr \leqslant 100$ and $-0.4 \leqslant m \leqslant 0.5$ have been given by the expressions [12]

$$Nu_{x,F} Re_x^{-1/2} = \alpha_F [1 + V_F] \tag{18}$$

where

$$\alpha_F = 0.464 Pr^{1/3}[1 + (0.0207/Pr)^{2/3}]^{-1/4} \tag{19}$$

$$V_F = m\{[0.44 + 5.0\exp(-6.0 Pr^{1/10})] - 0.18m\} \tag{20}$$

and

$$\overline{Nu}_{L,F} Re_L^{-1/2} = 2\alpha_F[1 + V_F]. \tag{21}$$

For pure free convection the local and average Nusselt numbers for $0.1 \leqslant Pr \leqslant 100$ and $-0.4 \leqslant m \leqslant 1.0$ can be correlated by the following expressions

$$Nu_{x,N} Gr_x^{*-1/6} = \alpha_N [1 + V_N] \tag{22}$$

where

$$\alpha_N = (Pr/6)^{1/6} \frac{Pr^{1/2}}{(0.12 + 1.195 Pr^{1/2})} \tag{23}$$

is taken from Armaly *et al.* [13] and, from the present results, V_N is given by

$$V_N = m/A1 - m^2/A2 + m^3/A3 \tag{24}$$

with

$$A1 = 9.120 \times 10^{-2} \ln(Pr) + 2.468,$$

$$A2 = 1.800 \times 10^{-1} \ln(Pr) + 6.170,$$

$$A3 = 3.370 \times 10^{-1} \ln(Pr) + 17.37. \tag{25}$$

The corresponding average Nusselt number is expressed by

$$\overline{Nu}_{L,N} Gr_L^{*-1/6} = \frac{6}{m+4} \alpha_N [1 + V_N]. \tag{26}$$

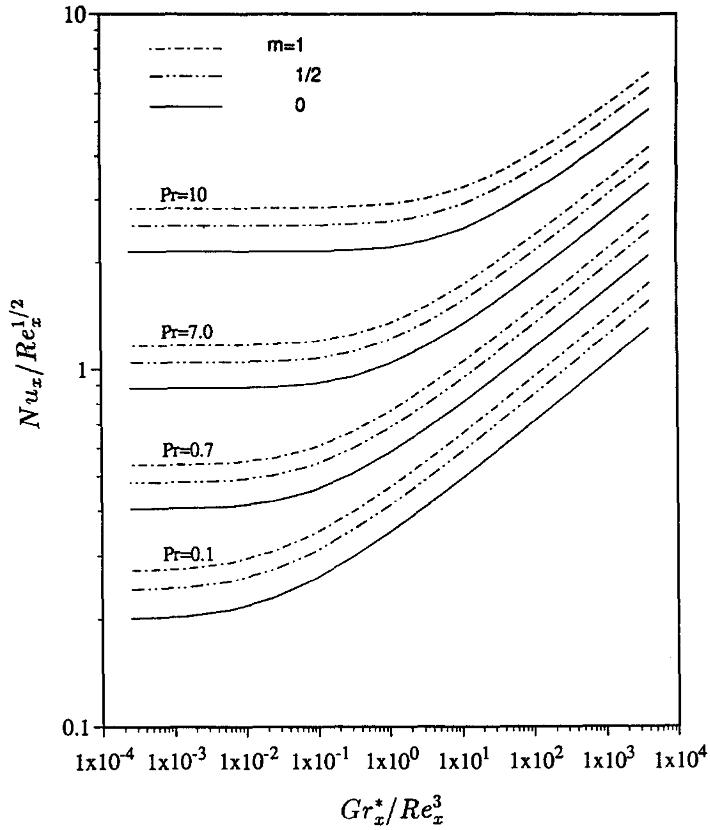

FIG. 3. $Nu_x Re_x^{-1/2}$ vs $Gr_x^* Re_x^{-3}$ for mixed convection.

Following Churchill [14], the correlation equation for Nusselt numbers in mixed convection can be expressed by the form

$$\left(\frac{Nu}{Nu_F}\right)^E = 1+\left(\frac{Nu_N}{Nu_F}\right)^E. \quad (27)$$

For the present study with a mixed convection parameter χ^*, the corresponding correlation equation for the mixed convection local Nusselt number can be represented by

$$\frac{Nu_x}{(Re_x^{1/2}+Gr_x^{*\,1/6})} = \left\{\left[\chi^*\left(\frac{Nu_{x,F}}{Re_x^{1/2}}\right)\right]^E + \left[(1-\chi^*)\left(\frac{Nu_{x,N}}{Gr_x^{*\,1/6}}\right)\right]^E\right\}^{1/E}. \quad (28)$$

It was found that the maximum difference between the correlated values from equation (28) and the calculated values is within 5% for $E = 3$.

The correlation equation for the mixed convection average Nusselt number can be similarly represented by

$$\frac{\overline{Nu}_L}{(Re_L^{1/2}+Gr_L^{*\,1/6})} = \left\{\left[\chi_L^*\left(\frac{\overline{Nu}_{L,F}}{Re_L^{1/2}}\right)\right]^E + \left[(1-\chi_L^*)\left(\frac{\overline{Nu}_{L,N}}{Gr_L^{*\,1/6}}\right)\right]^E\right\}^{1/E}. \quad (29)$$

The maximum difference between the correlated values from equation (29) and the calculated values from equations (15)–(17) is found to be within 10% for $E = 3$.

REFERENCES

1. J. R. Lloyd and E. M. Sparrow, Combined forced and free-convection flow on vertical surfaces, *Int. J. Heat Mass Transfer* **13**, 434–438 (1970).
2. N. Ramachandran, B. F. Armaly and T. S. Chen, Measurements and predictions of laminar mixed convection flow adjacent to a vertical surface, *J. Heat Transfer* **107**, 636–641 (1985).
3. A. Mucoglu and T. S. Chen, Mixed convection on inclined surfaces, *J. Heat Transfer* **101**, 422–426 (1979).
4. N. Ramachandran, B. F. Armaly and T. S. Chen, Measurements of laminar mixed convection flow adjacent to an inclined surface, *J. Heat Transfer* **109**, 146–151 (1987).
5. T. S. Chen, E. M. Sparrow and A. Mucoglu, Mixed convection in boundary layer flow on a horizontal plate, *J. Heat Transfer* **99**, 66–71 (1977).
6. N. Ramachandran, B. F. Armaly and T. S. Chen, Mixed convection over a horizontal plate, *J. Heat Transfer* **105**, 420–423 (1983).
7. A. Mucoglu and T. S. Chen, Mixed convection on a horizontal plate with uniform surface heat flux, *Proceedings of the 6th International Heat Transfer Conference*, Vol. 1, MC-15, pp. 85–90. Hemisphere, Washington, D.C. (1978).
8. M. S. Raju, X. Q. Liu and C. K. Law, A formulation of combined forced and free convection past horizontal and vertical surfaces, *Int. J. Heat Mass Transfer* **27**, 2215–2224 (1984).
9. W. Schneider and M. G. Wasel, Breakdown of the boundary-layer approximation for mixed convection above a

horizontal plate, *Int. J. Heat Mass Transfer* **28**, 2307–2313 (1985).
10. W. R. Risbeck, T. S. Chen and B. F. Armaly, Laminar mixed convection over horizontal flat plates with power-law variations in surface temperature, *Int. J. Heat Mass Transfer* **7**, 1859–1866 (1993).
11. B. Gebhart, *Heat Transfer* (2nd edn). McGraw-Hill, New York (1971).
12. H. Khouaja, T. S. Chen and B. F. Armaly, Mixed convection along slender vertical cylinders with variable surface heat flux, *Int. J. Heat Mass Transfer* **34**, 315–319 (1991).
13. B. F. Armaly, T. S. Chen and N. Ramachandran, Correlations for laminar mixed convection on vertical, inclined, and horizontal flat plates with uniform heat flux, *Int. J. Heat Mass Transfer* **30**, 405–408 (1987).
14. S. W. Churchill, A comprehensive correlating equation for laminar assisting, forced and free convection, *A.I.Ch.E. Jl* **23**, 10–16 (1977).

Pergamon

Int. J. Heat Mass Transfer. Vol. 37, No. 4, pp. 704–714, 1994

0017-9310/94 $6.00+0.00

Geometry dependent resistor model for predicting effective thermal conductivity of two phase systems

L. S. VERMA,† RAMVIR SINGH‡ and D. R. CHAUDHARY‡

† Dept. of Physics, M.S.J. College, Bharatpur (Rajasthan) 321 001, India
‡ Physics Department, University of Rajasthan, Jaipur 302 004, India

(*Received* 14 *January* 1991 *and in final form* 1 *March* 1993)

1. INTRODUCTION

THE KNOWLEDGE of the effective thermal conductivity of heterogeneous materials such as soils, ceramics, fiber reinforced materials and composites are becoming increasingly important in the technological developments and in many applications. Dependence of the effective thermal conductivity (*ETC*) of these materials on porosity, grain size and shape of the particles is also a matter of concern to engineers, architects and physicists. As it is not often possible to conduct experiments to study the effect of the above parameters on the *ETC*, a theoretical expression is needed to predict its value.

Though a large number of models exist in the literature, a general expression which can predict λ_e (*ETC*) of all kinds of two phase systems with the above parameters is still lacking.

The present paper is an effort to find a suitable expression to predict the *ETC* of various kinds of two phase systems. We have taken the electrical analog of various parameters to develop the expression. Equivalent thermal resistors formed out of the phases in form of parallel slabs are considered and the resistor model approach has been applied. The slabs are taken to be inclined to the direction of heat flow. By varying the angle of the slabs, the *ETC* of different two phase materials can be predicted. The angle has been defined in terms of various structural and thermal parameters.

2. THEORY

On the basis of phase averaging of temperature field, the following closure equations can be written for a two phase system. According to Hadley [1],

$$\nabla\langle T\rangle = \phi\langle\nabla T_1\rangle^1+(1-\phi)\langle\nabla T_2\rangle^2 \quad (1)$$

$$\frac{\lambda_e}{\lambda_1}\nabla\langle T\rangle = \phi\langle\nabla T_1\rangle^1+\frac{\lambda_2}{\lambda_1}(1-\phi)\langle\nabla T_2\rangle^2 \quad (2)$$

where $\langle\nabla T_1\rangle^1$ and $\langle\nabla T_2\rangle^2$ are average of the gradients in continuous phase and dispersed phase, respectively. ϕ is the porosity (volume fraction of continuous phase). These two equations contain three parameters $\nabla\langle T\rangle$, $\langle\nabla T_1\rangle^1$, and $\langle\nabla T_2\rangle^2$ and hence cannot be solved unless some relation connecting these parameters is assumed.

One possibility is $\langle\nabla T_1\rangle^1 = \langle\nabla T_2\rangle^2$, i.e. average temperature gradients in the two phases are equal. This condition is met in a collection of phase slabs, parallel to the direction of heat flow. This equality when put in equations (1) and (2) gives

$$\lambda_\parallel = [\phi\lambda_1+(1-\phi)\lambda_2]. \quad (3)$$

This is an expression for equivalent thermal conductivity of resistors arranged in parallel.

Similarly the assumption

$$\langle\nabla T_1\rangle^1 = \frac{\lambda_2}{\lambda_1}\langle\nabla T_2\rangle^2$$

when put in equations (1) and (2) gives,

$$\lambda_\perp = \left[\frac{\phi}{\lambda_1}+\frac{(1-\phi)}{\lambda_2}\right]^{-1}. \quad (4)$$

It is an expression for equivalent thermal conductivity of resistors arranged perpendicular to the heat flow. The above condition is equivalent to $\lambda_1\langle\nabla T_1\rangle^1 = \lambda_2\langle\nabla T_2\rangle^2$, i.e. the heat flux passing through different phases is the same. It is a situation met with the slabs perpendicular to the direction of heat flow.

Any model for a two phase system, having the *ETC* dependent on ϕ and λ_2/λ_1 can be represented by a general equation,

$$\langle\nabla T_1\rangle^1 = \left[f+\frac{\lambda_2}{\lambda_1}(1-f)\right]\langle\nabla T_2\rangle^2 \quad (5)$$

where f is a parameter lying between 0 and 1.

Here $\lambda_\parallel$ and $\lambda_\perp$ also represent upper and lower bounds of the effective thermal conductivity for a mixture.

Thus $\lambda_\parallel = (\lambda_e)_{max}$ and $\lambda_\perp = (\lambda_e)_{min}$.

We know that a porous medium is neither composed of slabs parallel to the heat flux nor perpendicular to it, yet the concept of the slabs is capable of predicting the maximum and minimum limits of the *ETC*. Therefore, it is proposed that the slabs of the continuous and dispersed phases, inclined to the heat flux may represent the *ETC* of the system.